METHODOLOGY

The advantages and challenges of non-invasive towed PILOT tags for free-ranging deep-diving megafauna

J. Fontes[1*], B. Macena[1], S. Solleliet-Ferreira[1], F. Buyle[2], R. Magalhães[3], T. Bartolomeu[3], N. Liebsch[4], C. Meyer[5] and P. Afonso[1]

Abstract

Background Biologging technologies have yielded new insights into the ecology and behaviour of elasmobranchs, but to date, most studies involve animal capture and restraint to attach tags. Capturing animals usually results in a period of atypical behaviour after release and is undesirable or simply not possible for large and vulnerable elasmobranchs such as mobulas and whale sharks. To avoid animal capture and restraint, we developed and tested two non-invasive multisensor towed tags. The use of towed packages creates additional data analytical challenges relative to fixed packages because towed devices wobble independently of animal movements. We present five examples, two mobulas (reef manta and sicklefin devil ray) and three sharks (blue, tiger and whale shark), to illustrate the advantages and challenges of this approach. We used animal-borne video to validate behavioural data derived from accelerometers and conducted an experiment to compare accelerometer data from attached and towed tags simultaneously deployed on a shark.

Results We used fluid dynamic models to calculate the added drag of towed devices on target species. We found that drag impact is acceptable for short-term tagging of large mobulas, but the drag penalty associated with the current camera tag design is greater than 5% for most mature blue sharks. Despite wobble effects, swimming behaviour (tail-beat and wing-stroke frequency) captured by towed accelerometers was consistent with those attached directly to the animal and with data from animal-borne video. Global Positioning System (GPS) sensors recorded up to 28 and 9 geolocations per hour of surface swimming by sicklefin devil ray and blue sharks, respectively.

Conclusions Towed tags with non-invasive attachments provide an effective alternative for acquiring high-resolution behaviour and environmental data without capturing and handling animals. This tool yields great potential to advance current knowledge of mobula ecology and behaviour without capture or invasive tagging.

Keywords Non-invasive, Bio-loggers, Sharks, Mobulas, Swimming behaviour

---

---

*Correspondence:
J. Fontes
Jorge.mr.fontes@uac.pt
Full list of author information is available at the end of the article

Fontes *et al. Animal Biotelemetry* 2022, **10**(1):39

Page 2 of 13

Background

Over the past several decades, electronic tagging has provided important new insights into the movement patterns, behaviour and physical environment of free-ranging marine animals [1]. This revolution has fuelled tremendous advances in scientific knowledge (e.g. [2–4]), improved our understanding of how environmental conditions are changing, and how these changes affect both the tagged animals and their ecosystems [5]. The interpretation of animal movement patterns is also a central piece of many ecological studies and a critical component of modern conservation research [6].

The need to gather behavioural and ecological data, unobtainable through direct observation, has driven a revolution in biologging sensor technology [7]. Modern biologging technologies that record both the internal (e.g. body temperature, heart rate) and external physical environment coupled with direct recording of behaviour from tri-axial sensors and animal-borne cameras offer a new approach for analysing the drivers of animal behaviour [1]. For example, the combined use of multiple sensors can reveal internal 'state' and behaviour, elucidate intraspecific interactions, reconstruct fine scale movements, and quantify local environmental conditions. However, with increasing sensor possibilities come new challenges: pinpointing the appropriate information to collect and determining the most efficient way to do so [7]. Despite the range of biologging sensors available today, 'off-the-shelf' devices are taxa specific (e.g. turtles, pelagic sharks, and large marine mammals) and typically combine a limited set of sensors designed to address a list of classic research questions. These universal questions have been summarized as: where is the animal going, how is the animal moving, what is the animal doing, and why is the animal moving [7]. Although there are multiple sensor combinations and design options available to tackle each question individually, the challenge becomes more substantial when two or more questions need to be addressed simultaneously. For example, if the relevant questions are "where is the animal going and how is it moving to get there?", it may be necessary to combine satellite and global navigation sensors with motion sensitive sensors, i.e. Inertial Measurement Unit (IMU), to reveal the pattern and intensity of movements, speed and direction.

A combination of IMU and depth data can also be used to reconstruct 3-dimensional (3D) animal movements when geolocation transmissions are limited or intermittent [8]. However, optimal sensor combinations are often not available 'off-the-shelf' (although see [9] and references therein), hence researchers must construct custom multisensor bundles (e.g. [10]) that typically require animal capture and restraint for attachment. Restraining animals creates a dilemma since a major goal of biologging studies is to minimize device impact on animal behaviour, energetics, and well-being [11]. Thus, non-invasive or low-impact tagging methods are desirable for ethical considerations and for ensuring that the collected data accurately reflect "non-tagged" behaviour [11]. An alternative to capturing and restraining marine animals, such as large pelagic sharks, is to use non-invasive fin clamps when attaching biologging devices to free-swimming individuals (e.g. [12]). However, some species, such as mobulas, lack large fins suitable for clamp attachment and alternatives such as spearing intramuscular anchors, are often not acceptable.

This is especially the case when studying species that are the focus of ecotourism operations and represent a significant source of income for local communities. Other iconic megafauna species are legally protected and the use of invasive, potentially detrimental, tag attachment methods are prohibited [13]. To overcome these restrictions, minimally invasive attachment methods, such as suctions cups with retention hooks, were developed to tag free-swimming mobulas. However, with the suction cup design, tag retention was limited to 5 h [14]. Recently, a non-invasive time-releasing harness was developed to increase the retention time of towed multisensor packages deployed on mobulas and pelagic sharks [15]. Towed devices offer a less invasive alternative to fixed devices however, current off-the-shelf towed multisensor tags typically contain a limited combination of sensors (e.g. pressure, temperature, light level, satellite geolocation) and are primarily designed for single deployments. We currently lack a towed deep-sea-going low drag multisensor tag that can simultaneously observe and measure essential behaviours using IMU, odometer, lighting and video, temperature, pressure as well as geolocation, and can be non-invasively attached to free-ranging animals. Here, we present two new non-invasive multisensor biologging tags, the i-Pilot and the G-Pilot, capable of reaching depths of 2000 m. We analysed their performance and validated the results for two mobulids (reef manta and sicklefin devil ray) and three sharks (tiger, blue and whale shark).

Methods

The Pilot tags are torpedo shaped, composed of two symmetrical floats (200 bar rated syntactic foam), held together by bolts and pins, to secure the electronic components and structural elements (Fig. 1A, B). The core of the i-Pilot contains a cylindrical titanium housing with an anterior view port and one rear deep-sea connector. The housing contains the camera, IMU unit, memory, pressure and water temperature sensors, battery, and common control board (PCB). The lighting system (red

Fontes *et al. Animal Biotelemetry* 2022, **10**(1):39

Page 3 of 13
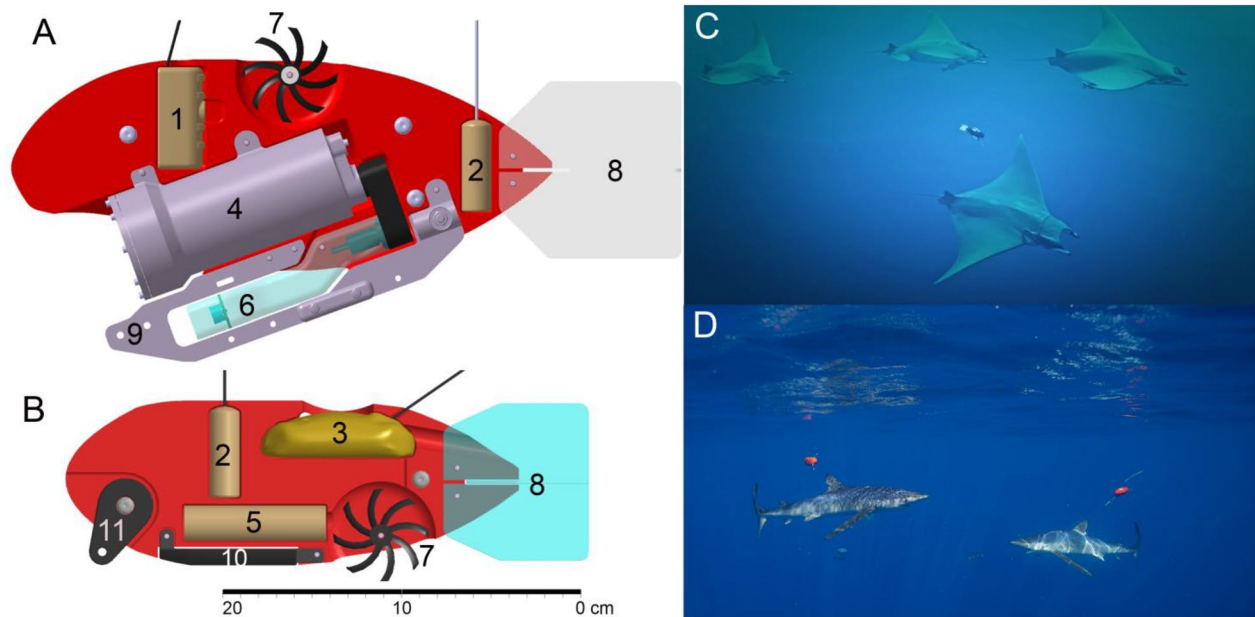
Fig. 1 Representation of the i-Pilot tag (**A**), G-Pilot tag (**B**), *Sicklefin devil ray* (250 cm disc width) tagged with the i-Pilot (**C**), and blue sharks (250 and 280 cm total length) tagged with G-Pilot tag (D). **1**—wildlife computers SPOT 363A transmitter; **2**—ATS VHF radio transmitter F1835B; **3**—wildlife computers SPLASH10-F-297A; **4**—titanium housing (camera, IMU, PCB. Battery, pressure and temperature sensors); **5**—CATS IMU; **6**—red LED; **7**—magnetic paddle wheel; **8**—stabilizing fins; **9**—tow connection; **10**—ballast; **11**—tow connection

LED) connects to the housing via a rear connector that is also used for charging, communicating, and downloading the data. The satellite and VHF transmitters are located on the dorsal section of the tag (Fig. 1A, B). A magnetic paddle wheel is located within a semi-circular flow chamber with half of the paddles exposed to the water flow. PVC clear vertical and horizontal rear fins are attached to the posterior end for stability. The G-Pilot tag contains one IMU unit, with pressure and water temperature sensors, one splash satellite tag (fastloc GPS), one VHF radio transmitter, one ventral magnetic paddle wheel, and stabilizing fins. The i-Pilot is 378 mm long, 120 mm wide, and weighs 1.76 kg in air with 0.23 kg of positive buoyancy. The G-Pilot is 294 mm long, 90 mm wide, and weights 0.77 kg with 0.2 kg of positive buoyancy.

While the use of animal-borne tags can impact the behaviour, energetics, and well-being of the animal, these effects are often ignored [11]. In particular, hydrodynamic drag, which can be considerable [5], and tag behaviour are seldom considered. On the other hand, it is also critical that the towed tags accurately measure the animal´s behaviour. We used computational fluid dynamics (CFD) models, to quantify drag increase, and controlled experiments to evaluate tag stability over a range of realistic tow speeds, and compared the behaviour recorded by the tags with concurrent video observations and behaviour data from attached and towed tags from the same animal.

Tag to animal drag

To quantify the relative drag increase resulting from the attachment of the Pilot tags, we used CFD models to simulate fluid flow over digital 3D models of a mobula, a blue shark and the tags themselves. We used blue shark and manta ray models available at https://www.3dcadbrowser.com/ as the basis of our 3D models. The base models were further improved using video and pictures of free-ranging animals along with measurements derived from photogrammetry and comments from the authors.

We simulated water flow velocities of between 0.5 and 4 ms^{-1} for devil rays (20 cm–300 cm disc widths, DW) and blue sharks (250 cm–350 cm total length, TL). We estimated the tag's drag for the same water flow velocities to calculate the increase in drag as the percentage of drag added by the tag with respect to body drag. This was done for each combination of tag, water velocity and body size.

Tag stability

Tags were towed from a boat with tags attached to a 15 kg wing depressor, to keep tags below propellor turbulence. Tags were towed for 120 s at each incremental speed, ranging from 0. 77 ms^{-1} to 6 ms^{-1}. GPS was used to measure tow speed. Tag stability was observed by a free diver positioned laterally to the predetermined boat route for each test.

Fontes *et al. Animal Biotelemetry* 2022, **10**(1):39

Page 4 of 13

Speed calculation

To calculate the relationship between the rotation frequency of the paddlewheel and the speed through the water we conducted multiple 25 m vertical drops, of the tags, while measuring the depth every 0.05 s (20 Hz). Speed was incrementally increased between drops by adding ballast weight. Tags were firmly attached to a vertical rod (250 cm) with ballast discs attached to the lower end. Divers verified that the drops were stable, and that no device spinning occurred. Magnetometers (detecting rotations of paddlewheel magnets) were set to record at 100 Hz.

Animal-borne tag performance and validation

Tag performance was evaluated by comparing IMU data with concurrent animal-borne video observations from; one 250 cm disk width (DW) reef manta (*Mobula alfredi*—tagged at Kona, Hawaii), one 300 cm (DW) sicklefin devil ray (*Mobula tarapacana*—tagged at the Princess Alice seamount Azores), one 300 cm total length (TL) blue shark (*Prionace glauca*, tagged at Faial island, Azores) and one 850 cm (TL) whale shark (*Rhincodon typus*—tagged at Sta. Maria islands, Azores). Tags were deployed by free divers using non-invasive attachment methods, self-releasing harness and fin clamp [15].

Shark harnesses were composed of 160 cm of monofilament line (1.40 mm) fitted through a 50 cm section of 3 mm diameter silicone tube to prevent abrasion. One end of the line was tied to a Galvanic Timed Release (GTR) link (International Fishing Devices Inc., Jupiter, Florida) and the other end was inserted through a 0.5 mm hole on a rectangular piece of soft rubber (2 mm thick, 10 mm × 5 mm), then through the second eye of the GTR, and finally through a second hole on the opposite end of the rubber piece. Prior to deployment the harness was secured to a U-shaped frame, via thin rubber bands, to hold the loop open and to keep the free diver´s hands away from the shark's mouth as the harness is fitted over the head. Once it is retained on the pectoral fins, the diver adjusts the harness to the correct girth. Upon total corrosion of the GTR (3 to 48 h according to the selected GTR) the harness and tag float to the surface, as the tag is positively buoyant. The mobula harness was composed of an elastic rope (6 mm thickness and 140 cm long), threaded through a metal ring, and attached to either end of a GTR forming a loop. A 100-cm-long piece of monofilament line was then tied to the metal ring and secured to the Pilot tag. Harnesses were deployed on free-swimming mobulas by free divers, by stretching the loop, with open arms in a U shape, to fit the harness around the head and rest it on the mobulids shoulders.

An off-the-shelf nylon clamp was fitted with a GTR release within the progressive tightening rack system to unlock and release the clamp after 3 to 24 h, according to the selected GTR [15]. A free diver attached the tag by securing the clamp on the posterior portion of the dorsal fin of a whale shark, leaving the tags to trail above the animals.

One 230 cm (TL) tiger shark (*Galeocerdo cuvier*), captured in Kaneohe bay (Hawaii), was restrained and double-tagged with both a towed i-Pilot tag, attached with a harness, and a high frequency tri-axial accelerometer tag attached directly to the pectoral fin [10]. In addition, five sicklefin devil rays (250–300 cm-DW) and five blue sharks (250–300 cm TL) were harness-tagged with G-Pilot tag in the Azores to evaluate Fastloc performance. Tags were programmed to record tri-axial acceleration (via accelerometer), angular velocity (via gyroscope) at 20 Hz, and magnetic field characteristics (via magnetometer) at 100 Hz. Depth and temperature were measured at 1 Hz. All tags were recovered for data retrieval using a combination of satellite transmitted ARGOS coordinates and radio telemetry or radio telemetry alone in the case of the tiger shark fixed package.

Handling and tagging activities in Hawaii were carried out in accordance with the animal use protocols of the University of Hawaii Institutional Animal Care and Use Committee (IACUC) and were approved under IACUC protocol #05-053. Tagging in the Azores were carried under the Azores government permits AMP/2017/013, AMP/2018/015, ELMAS-DRA/2019/05 and ELMAS-DRAM/2021/06.

Data analysis

Accelerometer and magnetometer data were extracted and analysed using Igor Pro-ver. 8.0 (Wavemetrics, Inc. Lake Oswego, USA), Ethnographer [16] and RStudio Ver. 1.1.453. Surging dynamic acceleration was used as proxy for wing-strokes and tail-beats because the Pilot tags are not rigidly attached to the body of the animal and can move laterally independent of the animal´s swaying acceleration. Swaying acceleration from the fixed package, on the tiger shark, was analysed following Nakamura et al. [17] and compared to the concurrent surging acceleration patterns from the towed i-Pilot tag.

Video files were synchronized and overlayed with the wavelet spectrogram of the surging acceleration from selected segments of dynamic acceleration data from each i-Pilot deployment, for direct comparison of swim patterns focal observations and accelerometer data. We used the VSDC Video Editor® Free Edition v6.8.3.343, to edit, synchronize and overlay video and wavelet spectrograms for visual inspection (supporting information).

Fontes *et al. Animal Biotelemetry* 2022, **10**(1):39

Page 5 of 13

Table 1 Estimated % of added drag at different water velocity flow rates (ms^{-1}) for the G-Pilot and i-Pilot tags deployed on sicklefin devil rays of different disc widths (DW)

Water velocity (ms^{-1})	G-Pilot/disk width (cm)		i-Pilot/disk width (cm)	
	250 (%)	300 (%)	250 (%)	300 (%)
0.5	2.5	1.7	7.9	5.5
0.75	2.4	1.7	8.0	5.6
1	2.4	1.7	8.2	5.6
2	2.3	1.6	8.8	6.1
4	2.3	1.6	9.2	6.3

Results

Drag and stability

Computer fluid dynamics model simulations indicate that the G-Pilot produces small (<5%) drag penalties for mobulas ranging in size from 250 and 300 m DW (Table 1). In contrast, the i-Pilot generates approximately 5–6% drag for a 300 cm mobula and up to 9% drag for smaller mobulas at very high velocities (Table 1). A significant portion of drag on the i-Pilot tag

is associated with the frontal flat view port (Additional file 1).

The G-Pilot tag generates added drag of approximately 5% for large (300–350 cm) blue sharks and up to 9% for 250 cm sharks (Table 2), whereas the i-Pilot tag increased drag by one third on a 250-cm shark and over 15% for the 350-cm shark.

Speed calibration (magnetometer and paddle wheel)

We found that the vertical velocity was linearly correlated with the magnetic paddle wheel rotation frequency, for both tags (i-Pilot $r^2 = 0.88$, $F_{(1,151)} = 1066.61$, $p \leq 0.0001$; G-Pilot $r^2 = 0.93$, $F_{(1,168)} = 2427.87$, $p \leq 0.0001$). The towed tag stability test showed that both tags remain stable up to speeds of 5 ms^{-1}. At 5.68 ms^{-1} the i-Pilot started spinning, precluding accurate speed estimation above this threshold. In contrast, the G-Pilot remained stable until the maximum tested speed of 6.66 ms^{-1}.

Geolocation G-pilot tag

G-pilot deployments on both mobulas and blue sharks produced 0.4 to 1.5 GPS locations per hour and 1.8 to

Table 2 Estimated % of added drag for the G-Pilot and the i-Pilot tags, simulated at different water velocity flow rates (ms^{-1}), for blue sharks of various total length, TL (m)

Water velocity (ms^{-1})	G-Pilot/body length (m)			i-Pilot/body length (m)		
	250 (%)	300 (%)	350 (%)	250 (%)	300 (%)	350 (%)
0.5	9.1	6.7	5.3	29.4	21.4	16.9
0.75	8.7	6.3	5.0	29.2	21.1	16.8
1	8.5	6.2	4.9	29.4	21.3	17.0
2	7.9	5.8	4.6	30.2	21.8	17.4
4	7.8	5.6	4.4	31.0	22.3	17.8

Table 3 Summary of fastloc® performance of the G-Pilot tag on *Sicklefin devil ray* (Mob) and *blue sharks* (BLU) in the Azores

ID and deployment duration (h)	Time at 0–1 m (%)	Time (h) at 0–1 m	Total FastLoc counts	FasLoc.h^{-1} (0–1 m)	FastLoc.h^{-1} (0-2000 m)
Mob-1 12.3 h	2.6	0.3	9	27.9	0.7
Mob-2 16.0 h	8.2	1.3	18	13.8	1.1
Mob-3 15.1 h	13.0	2.0	22	11.3	1.5
Mob-4 16.4 h	10.6	1.7	17	9.8	1.0
Mob-5 12.9 h	18.4	2.4	5	2.1	0.4
BLU-1 12.5 h	40	5.0	9	1.8	0.7
BLU2 17.5 h	16.0	2.8	9	3.2	0.5
BLU-3 13.5 h	13.1	1.8	7	4.0	0.5
BLU-4 27.9	2.7	0.8	22	9.2	0.8
BLU-5 38.3	17.5	6.6	20	3	0.5

Time at 0–1 m (%)—percent time spent between 0 and 1 m; time (h) at 0–1 m–time spent between 0 and 1 m; total FastLoc counts–number of successful fastloc locations acquired; FastLoc.h^{-1}(0–1 m)—number of successful fastloc locations per hour between 0 and 1 m; FastLoc.h^{-1}(0–2000 m)—total number of successful fastloc locations per hour

Fontes *et al. Animal Biotelemetry* 2022, **10**(1):39

Page 6 of 13
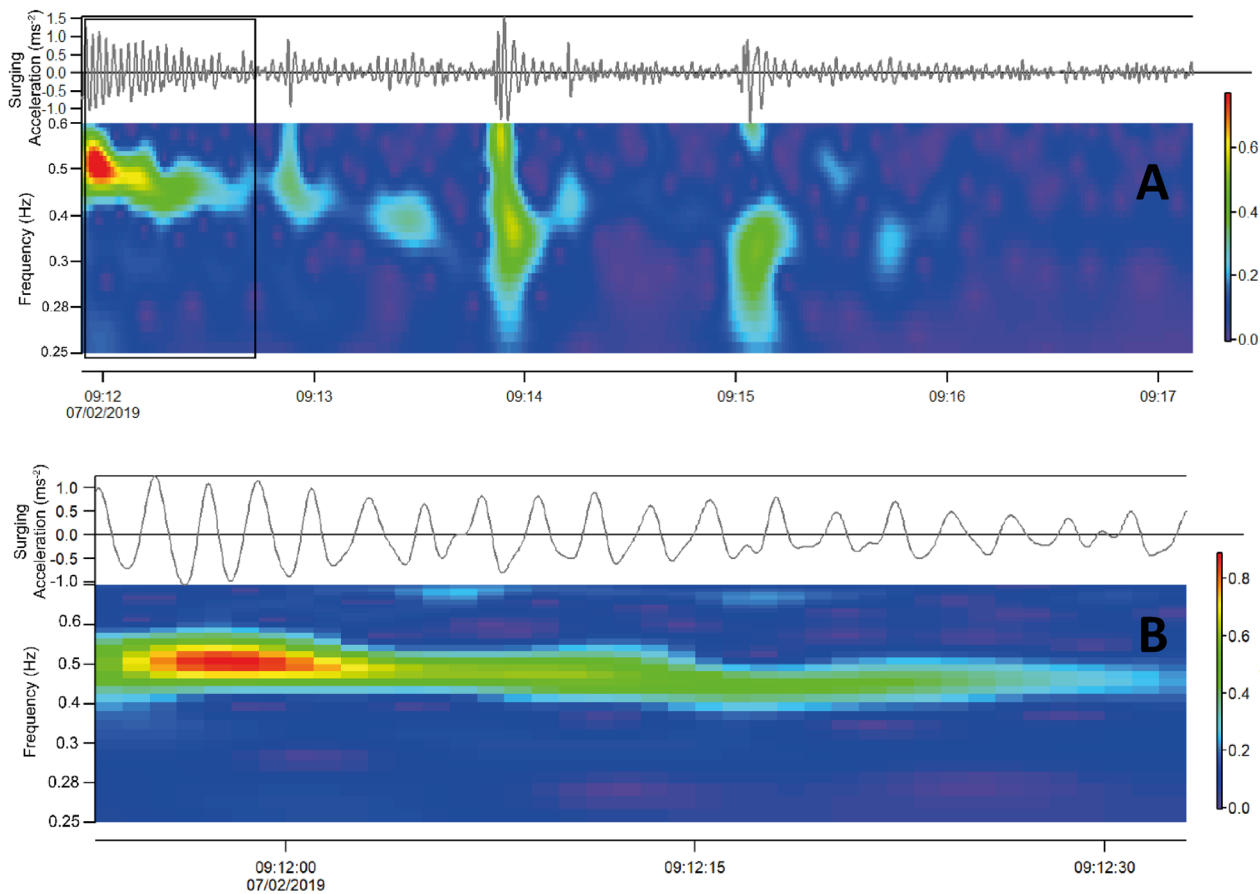
Fig. 2 Surging acceleration, and spectrogram of the surging acceleration during; **A** a 5-min segment of reef manta swimming data, **B** detail of the section delimited by the black rectangle in **A**. Warmer colours in the spectrogram represent stronger signals, whereas cooler colours represent weaker signals

28 locations per hour of time spent between 0 and 1 m depth (Table 3).

Swimming behaviour
Reef manta (M. alfredi)
The i-Pilot recorded reef manta swimming behaviours ranging from high frequency wing-strokes to gliding (Fig. 2A). Immediately following tag deployment, the accelerometer recorded the strongest surging acceleration, with high frequency (up to 5 Hz) and high-amplitude wing-strokes, consistent with burst swimming (warm colours, Fig. 2A). Both wing-stroke and amplitude decreased gradually over the first 45 s post-tagging (Fig. 2B). These patterns were corroborated by the concurrent animal-borne video (Additional file 2). Wing-stroke frequency and amplitude gradually decreased and for most of the deployment, alternated between low-frequency swimming, occasional short swim bursts and gliding (Additional file 3 represented by cool colours).

Sicklefin devil ray (M. tarapacana)
Figure 3A illustrates the surging acceleration during an ascent from circa 300 m depth to the surface, characterized by wing-stroke frequency of 0.25 Hz with variable wing-stroke amplitude (warm colours), followed by slight descent, characterized by low-amplitude wing-strokes and gliding (cold colours). Figure 3B presents a detail (box in Fig. 3A) of the ascent phase powered by 2.5 Hz wing-strokes, consistent with the concurrent video in Additional file 4.

Additional file 5 represents the variable swimming behaviour of sicklefin devil ray aggregations close to seafloor at a depth of 260 m.

Sicklefin devil ray swimming patterns recorded with the G-Pilot were similar to the patterns recorded by the i-Pilot. Figure 4 shows acceleration patterns consistent with gliding during both the descent and horizontal phase with ascents powered by variable wing-stroke frequency, ranging from roughly 2.5 to 0.3 Hz. Swimming

Fontes *et al. Animal Biotelemetry* 2022, **10**(1):39

Page 7 of 13
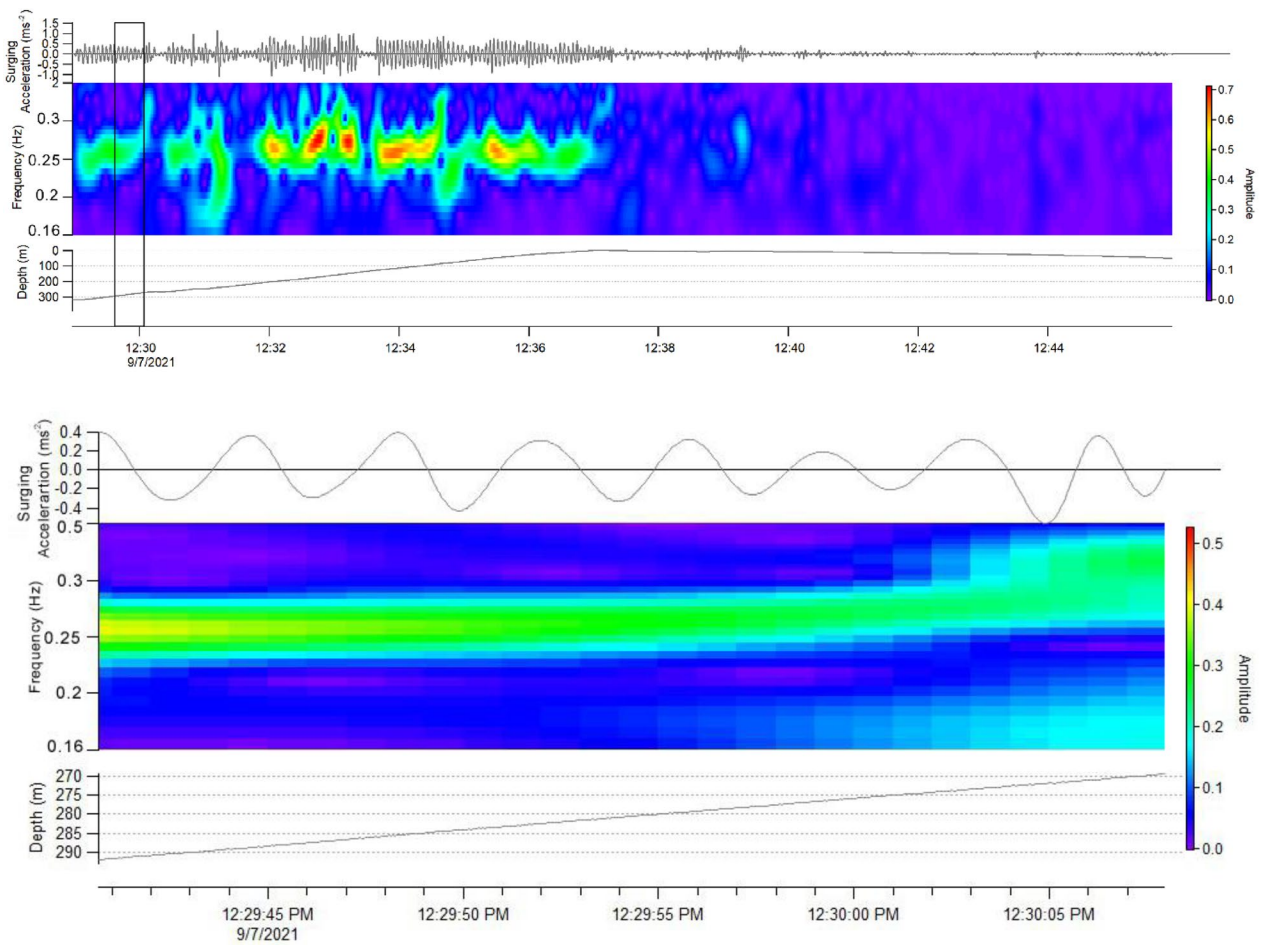
Fig. 3 Surging acceleration and spectrogram and depth from; **A** a 25-min ascent phase from a 250-cm sicklefin devil ray, **B** details of the section delimited by the black rectangle in **A**. Warmer colours in the spectrogram represent stronger signals, whereas cooler colours represent weaker signals
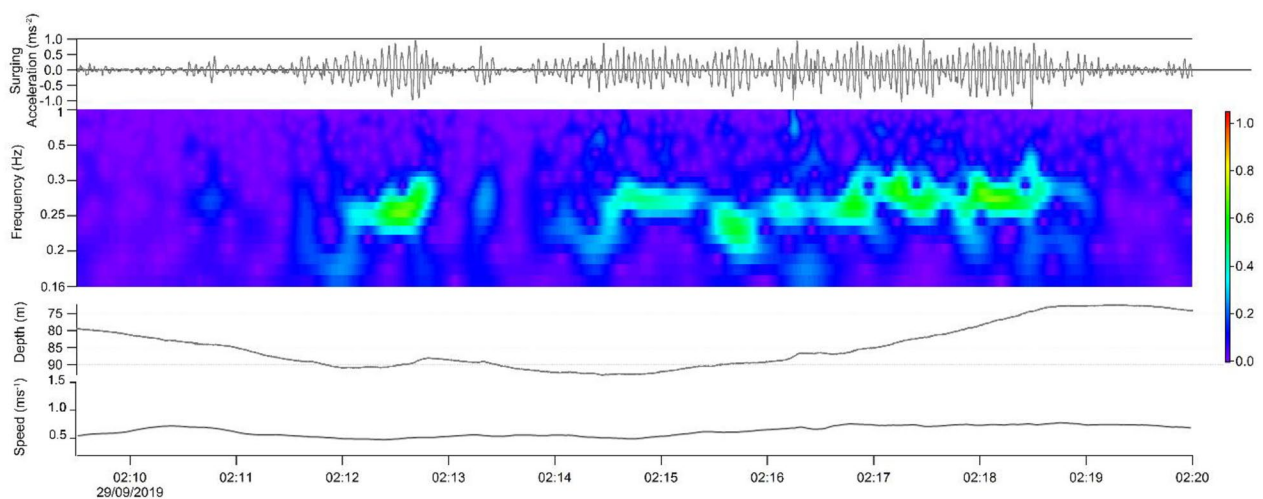
Fig. 4 Surging acceleration and spectrogram of the surging acceleration, depth and speed during of 10-min swimming by a 300-cm sicklefin devil ray. Warmer colours in the spectrogram represent stronger signals, whereas cooler colours represent weaker signals

Fontes *et al. Animal Biotelemetry* 2022, **10**(1):39

Page 8 of 13
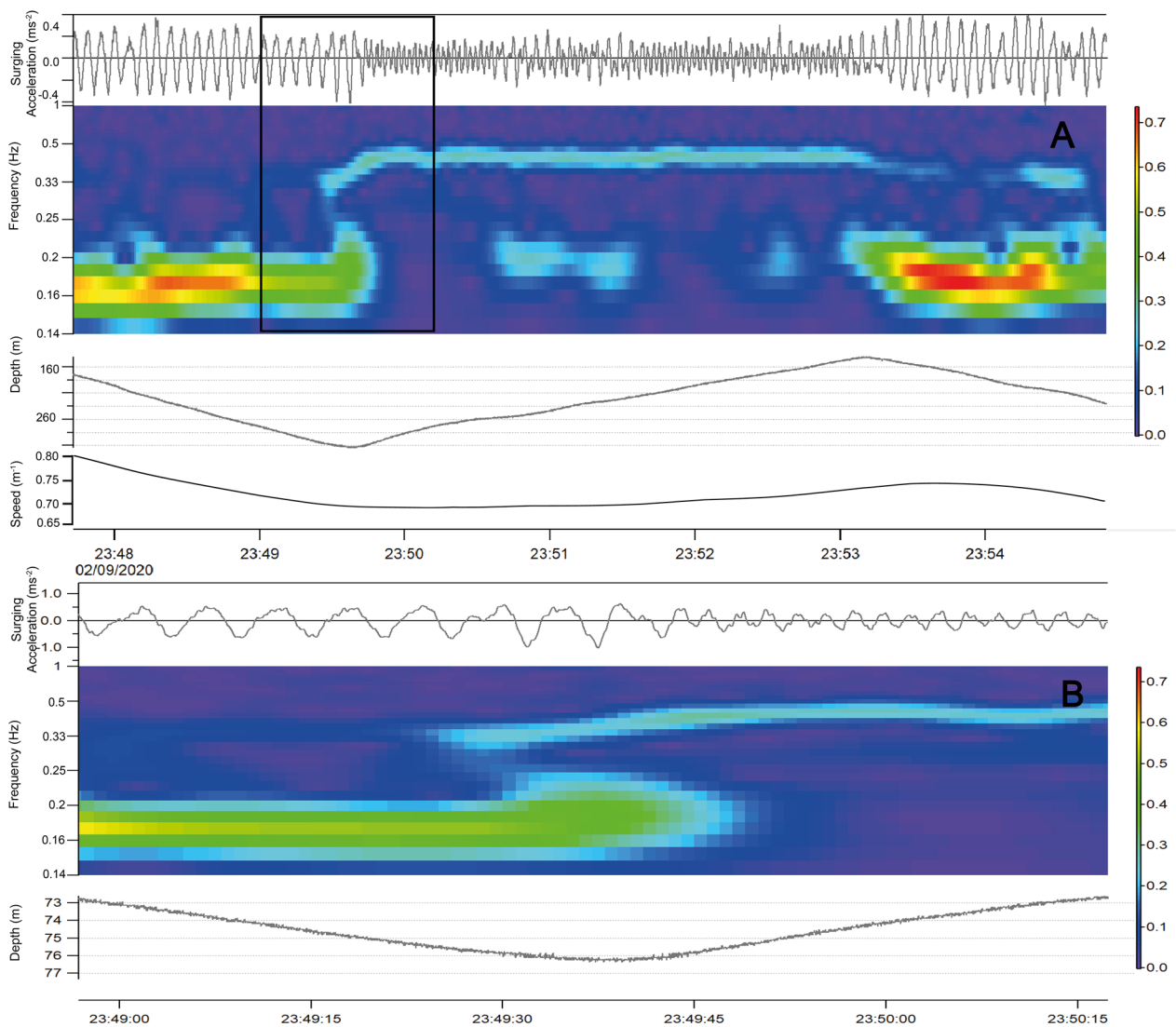
Fig. 5 Surging acceleration, depth, and speed over; **A** descent–ascent–descent swimming behaviour of a 280-cm blue shark, and **B** details of the section delimited by the black rectangle in **A**. Warmer colours in the spectrogram represent stronger signals, whereas cooler colours represent weaker signals

speed was also variable, ranging between 0.5 and 0.75 ms^{-1}, and tended to increase during the ascent along with an increase in wing-stroke frequency.

Blue shark (P. glauca)

Descent–ascent–descent behaviour, of a blue shark, at depth (250–310 m), is represented in Fig. 5. In this example, the surging acceleration frequency increased significantly from 0.16 Hz during descent to 0.45 Hz during the ascent phase. Additionally, a decrease in tail-beat amplitude is visible as the shark transitions from descent to ascent phase (Fig. 5A). These changes in surging acceleration are consistent with the animal-borne

video observations (Additional file 6), where head swaying movement (countering the tail-beat sway) patterns matched the surging acceleration patterns, for both frequency and amplitude.

Whale shark (R. typus)

The surging acceleration patterns from an 850-cm TL whale shark performing shallow Yo-Yo diving pattern, over a 35-min period, was characterized by descent glides followed by tail-stroke powered ascents (Fig. 6A). Figure 6B represents a portion of the ascent phase in which surging acceleration is relatively constant, at about

Fontes *et al. Animal Biotelemetry* 2022, **10**(1):39

Page 9 of 13
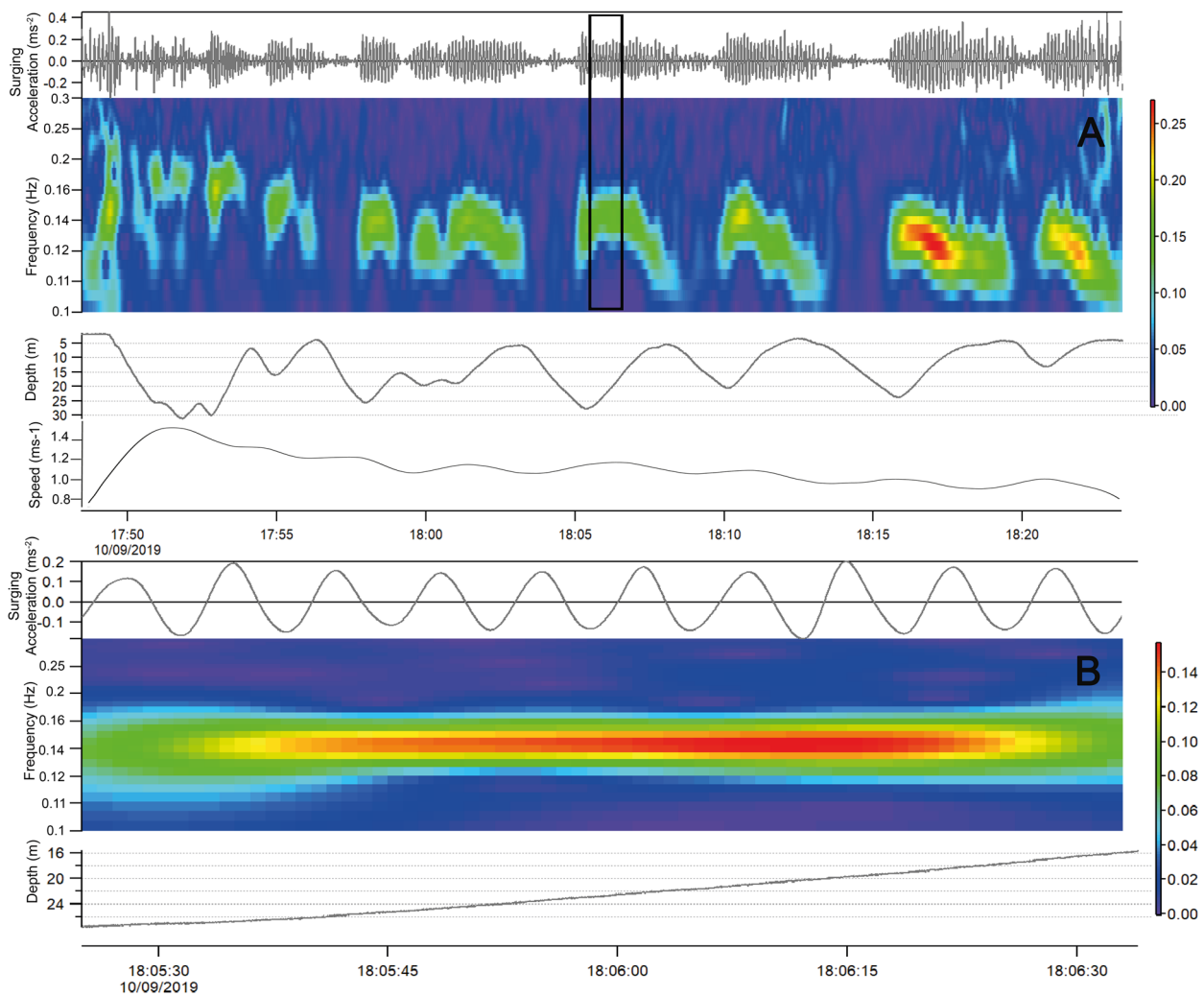
Fig. 6 Surging acceleration, depth and speed, **A** a 35-minute Yo-Yo behaviour segment of a 8500cm whale-shark, **B** detail of the section delimited by the black rectangle in **A**. Warmer colours in the spectrogram represent stronger signals, whereas cooler colours represent weaker signals

0.14 Hz, and aligns with the animal-borne video observations of swaying head movement, in counter-cycle with the tail-beat strokes (Additional file 7).

Tiger shark (G. cuvier) (towed vs fixed)
The surging and swaying acceleration patterns from simultaneously deployed, towed and fixed, accelerometers were similar. Both sensors recorded tail-beat frequency between 0.5 and 0.6 Hz during the first 210 min post-release, followed by a slight decrease and change in the dive profile (Fig. 7).

At higher resolution (3-min segment), both sensors capture comparable patterns of tail-beat frequency (ranging from approximately 0.4 to 0.7 Hz), reflecting similar relative changes in amplitude and frequency, even if the surge amplitude of the towed tag was slightly weaker (Fig. 8).

Discussion
Animal-borne tags (biologgers) have become powerful, widely used tools for investigating the behaviour and physiology of wild animals, and have advanced our understanding of the structure and function of global aquatic ecosystems (1). However, it is vital that these devices have minimal impact on the behaviour, energetics, and well-being of the animal for ethical reasons and to ensure that the resulting data accurately reflect "non-tagged" conditions [11]. In this context, we must consider the cost/benefit when planning tagging

Fontes *et al. Animal Biotelemetry* 2022, **10**(1):39

Page 10 of 13
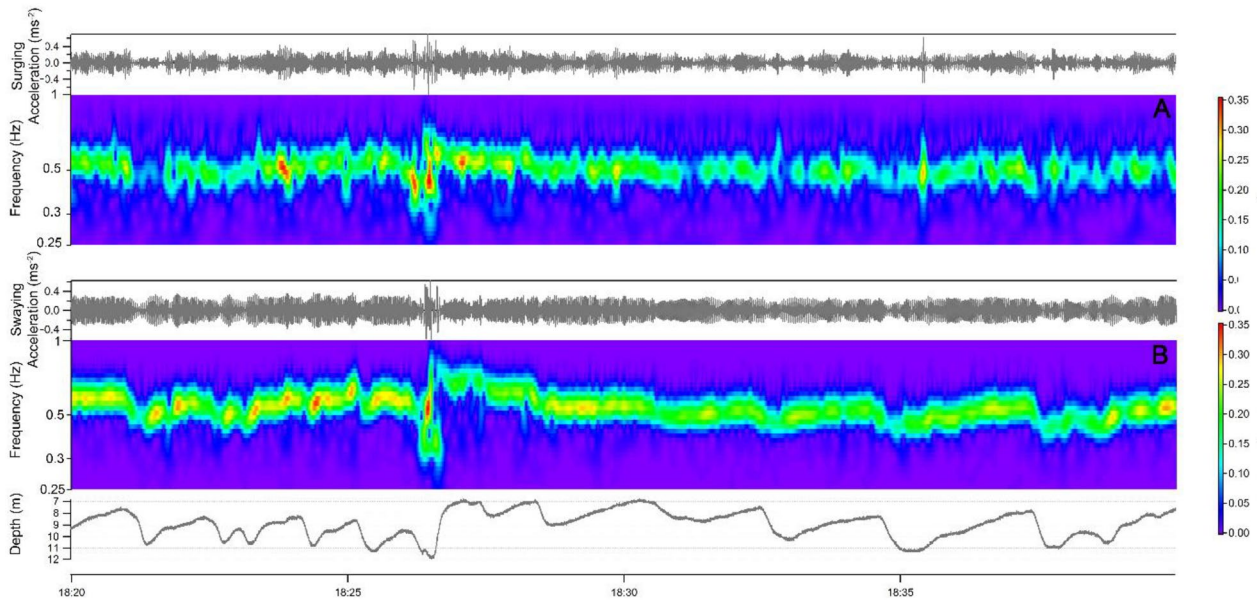
Fig. 7 Surging and swaying acceleration of a 230-cm tiger shark double-tagged with the i-Pilot (**A**) and an accelerometer/depth package attached to a pectoral fin (**B**). Warmer colours represent stronger signals and cooler colours represent weaker signals. Lower panel represents the dive profile (m)
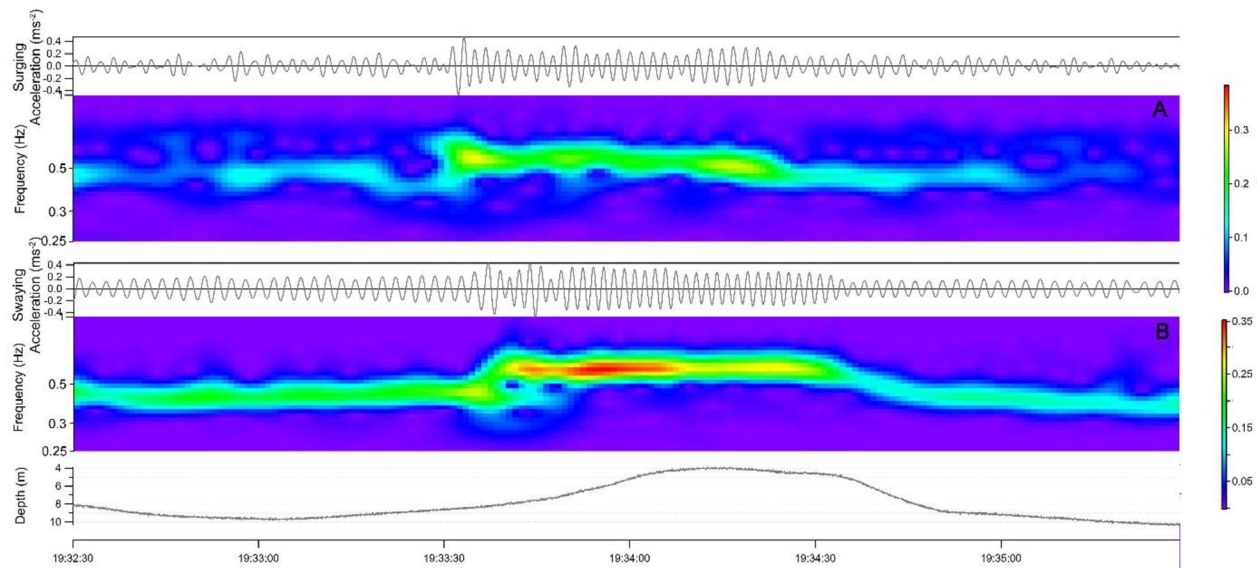
Fig. 8 Surging and swaying acceleration of a 230-cm tiger shark double tagged with i-Pilot (**A**) and accelerometer/depth package attached to a pectoral fin (**B**). Warmer colours represent stronger signals and cooler colours represent weaker signals. Bottom panel represents the dive profile (m)

experiments [18]. The widely accepted 5% rule [19], originally proposed for flying birds, focuses on the tag-to-animal weight ratio. However, hydrodynamic drag, which can be considerable [5], is seldom considered because quantifying relative drag increase is complex. In situ experimentation with the shape and position of tags on an experimental subject (or a model of it)

in wind or flume tunnels, or in captivity can be challenging, especially for large pelagic animals (but see [11, 20]). An alternative is to use computational fluid dynamics (CFD) models to estimate tag effects by simulating fluid flow over a tagged animal [18]. Ours is one of few available studies to examine the added drag of a new tag relative to the body size of the target

Fontes *et al. Animal Biotelemetry* 2022, **10**(1):39

Page 11 of 13

animals. Our simulation suggests both G-Pilot and i-Pilot tags produce minimal (up to 6%) drag increase when deployed on mobulas larger than 300 cm (DW), thus resulting in negligible impact on energetics and cost of transport during short term (12–48 h) deployments. Furthermore, large mobulas, including the sicklefin devil ray, typically host remoras (Echeneidae) (see Ref. [21] and Fontes personal observation– Additional file 8, [22]), which increase the cost of transport to some degree, and are thus adapted to manage variable drag loads.

Drag penalties for i-Pilot tags were estimated to be higher (17–31%) when deployed on blue sharks between 350 and 250 cm TL. However, these may be overestimates because our model assumed that sharks were stationary relative to the water flow, which can be 300% more hydrodynamically efficient than a swimming fish undulating body [23]. In addition, Watanabe et al. [24] recently reported that gliding behaviour accounted for only 10% and 20% of total descent duration of two tagged blue sharks, thus blue sharks will only use gliding during only 5 to 10% of the time when performing typical yoyo-diving [25]. The G-Pilot tags produce significantly lower drag penalties for blue sharks, close to the 5% threshold for animals larger than 250 cm, thus more suited to investigate the ecology of mature blue sharks.

Although it is crucial to minimize adverse tag effects on animals [5, 26], deployed devices must also collect valid data [27]. For example, towed tags must be sufficiently stable to collect useable high frequency tri-axial acceleration and angular velocity data [5, 28]. Both CFD results and field experiments confirm that the Pilot tags are stable up to speeds of 5 ms^{-1}, which is well above the sustained swim speed recorded for some of the fastest fishes such as, the giant Atlantic bluefin tuna (1.5 ms^{-1}, [29], the white shark (1.35 ms^{-1}[30], the sicklefin devil ray (0.6 ms^{-1}, Fig. 8), and the blue shark (0.75–0.5 ms^{-1}, Fig. 5) [24, 25]. The towed G-Pilot tag successfully quantified swimming performance, depth, and temperature while also yielding precise geolocations of tagged sharks and mobulas, and thus is a valuable tool for short-term studies where high-resolution data are required and fixed tags are not an option. Although, off-the-shelf, towed fastloc GPS tags are commercially available, these tags are expensive (ca. 5.000 US$), do not integrate accelerometer sensors, and are designed for a single long-term deployment. In addition, the performance of fastloc GPS technology has not yet been widely demonstrated for tracking mobulids (but see [31, 32]).

Most elasmobranch swimming behaviour studies utilize attached accelerometers because tail-beats are well correlated with tag sway acceleration (e.g. [8, 12, 30]). Our results showed that tail-beats from three different shark species are clearly represented in both surge and sway axes contradicting the assertions that anterior–posterior acceleration (surging acceleration) is minimal in swimming sharks [33]. Our results demonstrate that surging acceleration is superior to the swaying acceleration in accurately capturing the frequency and amplitude of tail-beats in sharks and wing-strokes mobulas equipped with towed Pilot tags, as towed tags can sway independent of the animal's movement. Our successful use of towed tags to characterize the complex swim patterns of mobulas establishes a new, low-impact method for investigating the poorly known ecology and behaviour of this group, in which most members are listed as endangered.

Challenges and limitations

Although a useful tool, towed tags have several inherent limitations compared to fixed devices. For example, the "wobble" associated with towed tags precludes accurate calculations of overall dynamic body acceleration (ODBA), a common proxy for energy expenditure derived from the sum of the absolute values of the dynamic accelerations from all three axes [34]. However, simple tail-stroke frequency has been well correlated with locomotor costs for seals (e.g. [35, 36]), fishes [37] and sharks [12, 33] suggesting that towed tags, which accurately capture this metric can still be effective tools for energetic studies of mobulas and other species.

Contrary to animal-attached tags, towed Pilot tags do not allow for realistic direct measurement of the animal´s pitch angle derived from the arcsine of the static acceleration in the surging (posterior–anterior) dimension [38] because the tag pitch can be different from the pitch of the animal during slow ascents since the tags are, positively buoyant (Fontes, personal observation). Nonetheless, average pitch may be derived from speed and vertical displacement averaged for a specific behaviour gate (ascent, descent or horizontal). The non-invasive deployment of the pilot tags using either the harness or fin clamp [15] requires reasonable freediving or SCUBA skills, depending on the behaviour of the target species.

Conclusions

Towed tags deployed via non-invasive harnesses provided clear measurements of swimming performance, along with behavioural and environmental data collected with minimal impact on sharks and mobulas. These characteristics make these devices valuable tools for acquiring crucial ecological and physiological information needed for effective conservation and management of sensitive endangered species such as mobulas. These tools can accelerate our current understanding of the fundamental ecology and behaviour of large mobulids in a context

Fontes *et al. Animal Biotelemetry*   2022, **10**(1):39

Page 12 of 13

where data on trophic ecology, locomotor behaviour and energetics from batoids are particularly scarce in comparison to data from teleost fishes and large sharks [13]. Future reductions in device size and drag, the addition of new environmental sensors (e.g. dissolved O_2), and cost reduction (e.g. using alternatives to expensive titanium housings) will further increase the utility of these devices by enabling them to be deployed on a wider size range of animals.

Abbreviations

IMU	Inertial measurement unit
PCB	Common control board (PCB)
LED	Light emitting diode
VHF	Very high frequency
PVC	Polyvinyl chloride
fastloc GPS	Fast location global positioning system
CFD	Computational fluid dynamic
DW	Disc width
TL	Total length

Supplementary Information

The online version contains supplementary material available at https://doi.org/10.1186/s40317-022-00310-1.

Additional file 1: SF1. The vorticity field associated with the i-Pilot tag (upper panel) and G-Pilot tags (lower panel) form CFD model with water flow at 0.5 ms-1 (note the different size scales on top and lower panels).

Additional file 2: SF2. Reef manta burst swimming.

Additional file 3: SF3. Reef manta gliding.

Additional file 4: SF4. Sicklefin devil ray ascent.

Additional file 5: SF5. Sicklefin devil ray deep bottom dwelling.

Additional file 6: SF6. Blue shark decent–ascent.

Additional file 7: SF7. Whale shark shallow ascent behaviour.

Additional file 8: Sicklefin devil ray (*Mobula tarapacana*) with G-Pilot tag and remoras (*Remora remora*) attached.

Availability of data and materials

The datasets used and/or analysed during the current study are available from the corresponding author on reasonable request.

Declarations

Ethics approval and concent to participate

"Handling and tagging activities were carried out in accordance with the animal use protocols of the University of Hawaii Institutional Animal Care and Use Committee (IACUC protocol #05-053) and Azores government permits AMP/2017/013, AMP/2018/015, ELMAS-DRA/2019/05 204 and ELMAS-DRAM/2021/06."

Consent for publication

Not applicable.

Competing interests

The authors declare that they have no competing interests.

Author details

[1]Institute of Marine Sciences - Okeanos, University of the Azores, Rua Professor Doutor Frederico Machado 4, 9901-862 Horta, Portugal. [2]Nektos.Net, Brussels, Belgium. [3]Centre for Engineering and Product Development, Matosinhos, Portugal. [4]Customized Animal Tracking Solutions, Caloundra, Australia. [5]Hawai'i Institute of Marine Biology, Hawaii University at Manoa, P. O. Box 1346, Kaneohe, HI, USA.

References

1. Hussey NE, Kessel ST, Aarestrup K, Cooke SJ, Cowley PD, Fisk AT, et al. Aquatic animal telemetry: a panoramic window into the underwater world. Science. 2015;348(6240):1255642.
2. Braun CD, Gaube P, Sinclair-Taylor TH, Skomal GB, Thorrold SR. Mesoscale eddies release pelagic sharks from thermal constraints to foraging in the ocean twilight zone. Proc Natl Acad Sci. 2019;116(35):17187–92.
3. Thorrold SR, Afonso P, Fontes J, Braun CD, Santos RS, Skomal GB, et al. Extreme diving behaviour in devil rays links surface waters and the deep ocean. Nature Commun. 2014;5:1–7.
4. Yoshino K, Takahashi A, Adachi T, Costa DP, Robinson PW, Peterson SH, et al. Acceleration-triggered animal-borne videos show a dominance of fish in the diet of female northern elephant seals. J Exp Biol. 2020;223(5):jeb212936.
5. Kay WP, Naumann DS, Bowen HJ, Withers SJ, Evans BJ, Wilson RP, et al. Minimizing the impact of biologging devices: using computational fluid dynamics for optimizing tag design and positioning. Methods Ecol Evol. 2019;10(8):1222–33.
6. Harcourt R, Sequeira A, Zhang X, Roquet F, Komatsu K, Heupel M. Animal-borne telemetry: an integral component of the ocean observing toolkit. Front Mar Sci. 2019;6(326):2020.
7. Williams HJ, Taylor LA, Benhamou S, Bijleveld AI, Clay TA, de Grissac S, et al. Optimizing the use of biologgers for movement ecology research. J Anim Ecol. 2020;89(1):186–206.
8. Andrzejaczek S, Gleiss AC, Lear KO, Pattiaratchi CB, Chapple TK, Meekan MG. Biologging tags reveal links between fine-scale horizontal and vertical movement behaviors in tiger sharks (*Galeocerdo cuvier*). Front Mar Sci. 2019;6:229.
9. Skubel RA, Wilson K, Papastamatiou YP, Verkamp HJ, Sulikowski JA, Benetti D, et al. A scalable, satellite-transmitted data product for monitoring

Fontes *et al. Animal Biotelemetry* 2022, **10**(1):39

Page 13 of 13

high-activity events in mobile aquatic animals. Anim Biotelemetry. 2020;8(1):1–14.

10. Royer M, Maloney K, Meyer C, Cardona E, Payne N, Whittingham K, et al. Scalloped hammerhead sharks swim on their side with diel shifts in roll magnitude and periodicity. Anim Biotelemetry. 2020;8(1):1–12.

11. Rosen DA, Gerlinsky CG, Trites AW. Telemetry tags increase the costs of swimming in northern fur seals, *Callorhinus ursinus*. Mar Mamm Sci. 2018;34(2):385–402.

12. Gleiss AC, Norman B, Liebsch N, Francis C, Wilson RP. A new prospect for tagging large free-swimming sharks with motion-sensitive data-loggers. Fish Res. 2009;97(1–2):11–6.

13. Stewart JD, Jaine FR, Armstrong AJ, Armstrong AO, Bennett MB, Burgess KB, et al. Research priorities to support effective manta and devil ray conservation. Front Mar Sci. 2018;5:314.

14. Stewart JD, Smith TT, Marshall G, Abernathy K, Fonseca-Ponce IA, Froman N, et al. Novel applications of animal-borne Crittercams reveal thermocline feeding in two species of manta ray. Mar Ecol Prog Ser. 2019;632:145–58.

15. Fontes J, Baeyaert J, Prieto R, Graça G, Buyle F, Afonso P. New non-invasive methods for short-term electronic tagging of pelagic sharks and rays. Mar Biol. 2018;165(2):34.

16. Sakamoto KQ, Sato K, Ishizuka M, Watanuki Y, Takahashi A, Daunt F, et al. Can ethograms be automatically generated using body acceleration data from free-ranging birds? PLoS ONE. 2009;4(4): e5379.

17. Nakamura I, Watanabe YY, Papastamatiou YP, Sato K, Meyer CG. Yo-yo vertical movements suggest a foraging strategy for tiger sharks *Galeocerdo cuvier*. Mar Ecol Prog Ser. 2011;424:237–46.

18. Kyte A, Pass C, Pemberton R, Sharman M, McKnight JC. A computational fluid dynamics (CFD) based method for assessing the hydrodynamic impact of animal borne data loggers on host marine mammals. Mar Mamm Sci. 2019;35(2):364–94.

19. Casper RM. Guidelines for the instrumentation of wild birds and mammals. Anim Behav. 2009;78(6):1477–83.

20. Van der Hoop JM, Fahlman A, Shorter KA, Gabaldon J, Rocho-Levine J, Petrov V, et al. Swimming energy economy in bottlenose dolphins under variable drag loading. Front Mar Sci. 2018;5:465.

21. Nicholson-Jack AE, Harris JL, Ballard K, Turner KM, Stevens GM. A hitchhiker guide to manta rays: patterns of association between *Mobula alfredi*, *M. birostris*, their symbionts, and other fishes in the Maldives. PLoS ONE. 2021;16(7):0253704.

22. Becerril-García E, Gutiérrez-Ortiz M, Preciado-González P, Ayala-Bocos A. Presence of *Remora remora* on Mobula birostris in Revillagigedo National Park, Mexico. Mar Freshw Res. 2019;71(3):414–7.

23. Weihs D. Energetic advantages of burst swimming of fish. J Theor Biol. 1974;48(1):215–29.

24. Watanabe YY, Nakamura I, Chiang W-C. Behavioural thermoregulation linked to foraging in blue sharks. Mar Biol. 2021;168(11):1–10.

25. Carey FG, Scharold JV. Movements of blue sharks (*Prionace-Glauca*) in depth and course. Mar Biol. 1990;106(3):329–42.

26. Jones TT, Van Houtan KS, Bostrom BL, Ostafichuk P, Mikkelsen J, Tezcan E, et al. Calculating the ecological impacts of animal-borne instruments on aquatic organisms. Methods Ecol Evol. 2013;4(12):1178–86.

27. Whitney NM, Lear O, Gleiss AC, Payne N, White CF. Advances in the application of high-resolution biologgers to elasmo-branch fishes. Shark Res. 2018;3:45–70.

28. Gleiss AC, Norman B, Wilson RP. Moved by that sinking feeling: variable diving geometry underlies movement strategies in whale sharks. Funct Ecol. 2011;25(3):595–607.

29. Gleiss AC, Schallert RJ, Dale JJ, Wilson SG, Block BA. Direct measurement of swimming and diving kinematics of giant Atlantic bluefin tuna (*Thunnus thynnus*). Roy Soc Open Sci. 2019;6(5):190203.

30. Watanabe YY, Payne NL, Semmens JM, Fox A, Huveneers C. Swimming strategies and energetics of endothermic white sharks during foraging. J Exp Biol. 2019;222(4):185603.

31. Braun CD, Skomal GB, Thorrold SR, Berumen ML. Movements of the reef manta ray (*Manta alfredi*) in the Red Sea using satellite and acoustic telemetry. Mar Biol. 2015;162(12):2351–62.

32. Lassauce H, Chateau O, Erdmann MV, Wantiez L. Diving behavior of the reef manta ray (Mobula alfredi) in New Caledonia: more frequent and deeper night-time diving to 672 meters. PLoS ONE. 2020;15(3):1.

33. Gleiss AC, Dale JJ, Holland KN, Wilson RP. Accelerating estimates of activity-specific metabolic rate in fishes: testing the applicability of acceleration data-loggers. J Exp Mar Biol Ecol. 2010;385(1–2):85–91.

34. Gleiss AC, Wilson RP, Shepard EL. Making overall dynamic body acceleration work: on the theory of acceleration as a proxy for energy expenditure. Methods Ecol Evol. 2011;2(1):23–33.

35. Jeanniard-du-Dot T, Trites AW, Arnould JP, Speakman JR, Guinet C. Flipper strokes can predict energy expenditure and locomotion costs in free-ranging northern and Antarctic fur seals. Sci Rep. 2016;6(1):1–12.

36. Williams TM, Fuiman LA, Horning M, Davis RW. The cost of foraging by a marine predator, the Weddell seal *Leptonychotes weddellii*: pricing by the stroke. J Exp Biol. 2004;207(6):973–82.

37. Wilson S, Hinch S, Eliason E, Farrell A, Cooke S. Calibrating acoustic acceleration transmitters for estimating energy use by wild adult Pacific salmon. Comp Biochem Physiol Mol Integr Physiol. 2013;164(3):491–8.

38. Sato K, Mitani Y, Cameron MF, Siniff DB, Naito Y. Factors affecting stroking patterns and body angle in diving Weddell seals under natural conditions. J Exp Biol. 2003;206(9):1461–70.

Publisher's Note